Regulatory Mechanisms in Biosystems

ISSN 2519-8521 (Print)
ISSN 2520-2588 (Online)
Regul. Mech. Biosyst.

Comparative analysis of ACE2 and antibody binding affinities of post-pandemic SARS-CoV-2 variants

M. Peka*, **, A. Saienko**, S. Korinnyi**

**V. N. Karazin Kharkiv National University, Kharkiv, Ukraine*
***Institute of Pig Breeding and Agroindustrial Production of the National Academy of Agrarian Sciences of Ukraine, Poltava, Ukraine*

Article info

Received 03.03.2026
Received in revised form 09.04.2026
Accepted 06.05.2026

V. N. Karazin Kharkiv National University, Svobody sq., 4, Kharkiv, 61022, Ukraine. Tel.: +38-057-707-55-00. E-mail: pekapoltava@gmail.com

Institute of Pig Breeding and Agroindustrial Production of the National Academy of Agrarian Sciences of Ukraine, Shvedska Mohyla st., 1, Poltava, 36009, Ukraine. Tel.: +38-063-395-55-31. E-mail: pigbreeding@ukr.net

Peka, M., Saienko, A., & Korinnyi, S. (2026). Comparative analysis of ACE2 and antibody binding affinities of post-pandemic SARS-CoV-2 variants. Regulatory Mechanisms in Biosystems, 17(3), e26052. doi:10.15421/0226052

Post-pandemic evolution of severe acute respiratory syndrome coronavirus 2 (SARS-CoV-2), the causative agent of COVID-19, is characterized by the continuous emergence of variants carrying numerous mutations within the receptor-binding domain (RBD) of the spike protein. These mutations may alter viral affinity for the angiotensin-converting enzyme 2 (ACE2) receptor and neutralizing antibodies, thereby influencing transmissibility and immune evasion. The aim of this study was to perform a comparative *in silico* analysis of the binding affinities of major post-pandemic SARS-CoV-2 variants toward the human ACE2 receptor and a reference neutralizing antibody. Mutational profiles of XBB.1.5, XBB.1.16, EG.5, BA.2.86, JN.1, KP.3.1.1, NB.1.8.1, XFG, and BA.3.2 lineages were analyzed, structural models of RBD-ACE2 and RBD-antibody complexes were generated, and binding free energies were estimated. Molecular dynamics simulations were performed for selected complexes containing RBDs of the XBB.1.5 and BA.3.2.2 variants, as well as the wild-type SARS-CoV-2, and structural stability, conformational dynamics, hydrogen bonding, and free energy landscapes were evaluated. All analyzed post-pandemic variants formed less stable complexes with the reference antibody than the wild-type virus, indicating a general evolutionary trend toward enhanced immune evasion. However, only a subset of variants demonstrated enhanced affinity for ACE2. Molecular dynamics simulations demonstrated that post-pandemic variants acquired distinct conformational dynamics and metastable states compared with the wild-type virus. In particular, XBB.1.5 and BA.3.2.2 formed more stable complexes with ACE2 and less stable complexes with the antibody than the wild-type virus. These findings suggest that post-pandemic SARS-CoV-2 evolution is driven predominantly by optimization of immune evasion while preserving effective receptor interaction. The study also demonstrates that the applied computational workflow may be useful for rapid characterization of newly emerging SARS-CoV-2 variants.

Keywords: COVID-19; virus; bioinformatics; *in silico* methods; molecular dynamics, mutation, receptor binding.

Introduction

Severe acute respiratory syndrome coronavirus 2 (SARS-CoV-2) is a member of the *Coronaviridae* family (Rathore & Ghosh, 2020; Rabaan et al., 2023) and the causative agent of COVID-19 (Ayenigbara, 2020; Pal et al., 2020). In 2020, the virus caused a global pandemic with profound social (Saladino et al., 2020; Naveed et al., 2024) and economic (Pak et al., 2020; Sun et al., 2024) consequences. Although the World Health Organization (WHO) declared the end of the COVID-19 public health emergency of international concern (PHEIC) in May 2023 (Burki, 2023; Sarker et al., 2023), COVID-19 continues to remain a global health concern with substantial impacts on human health (Chung et al., 2024; Santo et al., 2025). Following the end of the pandemic phase, several SARS-CoV-2 variants, including XBB.1.5 (Islam et al., 2023), XBB.1.16 (Pourriyahi et al., 2024), EG.5 (Yadav et al., 2023), BA.2.86 (Wang et al., 2023), JN.1 (Yang et al., 2024), KP.3.1.1 (Shi et al., 2025), NB.1.8.1 (Uriu et al., 2025), XFG (Azhar et al., 2026), and BA.3.2 (Fourati & Loubet, 2026) became prevalent in different regions of the world or caused localized outbreaks (Alhamlan & Al-Qahtani, 2025; Uraki et al., 2026). Although none of these variants were classified as variants of concern (VOCs) during the post-pandemic period, some were designated as variants of interest (VOIs) or variants under monitoring (VUMs) according to WHO and European Centre for Disease Prevention and Control (ECDC) criteria, reflecting their epidemiological relevance and the need for continued surveillance (Ambrosio et al., 2022; Andre et al., 2023).

The key epidemiological characteristics of SARS-CoV-2 variants include transmissibility, virulence, immune evasion, and susceptibility to therapeutic interventions (Cocherie et al., 2022; Carabelli et al., 2023). Viral evolution and the accumulation of mutations may provide selective advantages in all of these aspects. In particular, mutations within the spike glycoprotein play a central role in these processes (Carabelli et al., 2023; Zabidi et al., 2023). For example, the Omicron variant gained a substantial evolutionary advantage over preceding variants through the rapid accumulation of mutations in the spike protein, resulting in increased transmissibility and reduced neutralizing antibody efficacy (Parsons & Acharya, 2023; Liu et al., 2024b). Omicron-derived lineages continue to predominate during the post-pandemic period (Kung et al., 2025; Souza et al., 2025).

The presence of a surface spike glycoprotein (S protein) is a characteristic feature of both SARS-CoV-2 and coronaviruses in general (Ou et al., 2020; Saadi et al., 2021; Banerjee et al., 2022). The S protein consists of two subunits: S1, which contains the receptor-binding domain (RBD) responsible for receptor recognition, and S2, which mediates membrane fusion (Huang et al., 2020; Walls et al., 2020). Whereas the S1 subunit is relatively variable and largely determines receptor tropism, the S2 subunit contains more conserved sequences shared among coronaviruses (Lu et al., 2023; Bocquet-Garçon, 2024). The primary cellular receptor for SARS-CoV-2 is angiotensin-converting enzyme 2 (ACE2), and interaction with ACE2 represents a critical step in viral entry and COVID-19 pathogenesis (Bourgonje et al., 2020; Wang et al., 2020). Consequently, the accumulation of mutations that increase affinity for ACE2 may confer an evolutionary advantage by enhancing viral infectivity and transmission (Markov et al., 2023; Ataya et al., 2025).

Another major mechanism by which mutations may facilitate viral spread is immune evasion (Carabelli et al., 2023; Markov et al., 2023). Despite extensive efforts to develop antiviral therapies against SARS-CoV-2, pharmacological treatment options remain limited (Yaghoubi et al., 2021; Murmu et al., 2024; Alves et al., 2025; Soares et al., 2025), and vaccination continues to represent the primary strate-

gy for COVID-19 prevention (Tradigo et al., 2023). However, ongoing viral evolution and the continuous accumulation of mutations in the S protein pose substantial challenges for both vaccine efficacy (Faraji et al., 2024) and therapeutic development (Hwang et al., 2022; Aboul-Fotouh et al., 2023). The S protein, particularly the RBD, remains the principal target for vaccines and many therapeutic agents directed against COVID-19 (Guan et al., 2023; Islam, 2023). At the same time, under selective pressure exerted by host immunity, the majority of mutations emerging in novel SARS-CoV-2 variants are concentrated within the S1 subunit (Mengist et al., 2021; Lu et al., 2023; Magazine et al., 2024).

Consequently, investigating the interactions of the SARS-CoV-2 RBD with both the ACE2 receptor and neutralizing antibodies remains an important objective during the post-pandemic period. In this context, *in silico* approaches are particularly valuable because they enable rapid assessment of the effects of mutations present in newly emerging variants on binding affinity toward ACE2 and antibodies. Therefore, the aim of this study was to perform a comparative *in silico* analysis of the binding affinities of post-pandemic SARS-CoV-2 variants in complexes with both the ACE2 receptor and antibodies.

Materials and methods

A comparative analysis was conducted between the WT SARS-CoV-2 virus and variants classified as VOIs during the post-pandemic period (2023–2026): XBB.1.5, XBB.1.16, EG.5, BA.2.86, and JN.1, as well as variants classified as VUMs at the time of the study in 2026: KP.3.1.1, NB.1.8.1, XFG, and BA.3.2 sublineages (BA.3.2.1 and BA.3.2.2). Mutational profiles of the studied variants within the RBD of the S protein were determined based on data from open databases (Chen et al., 2022; Gangavarapu et al., 2023; Tsueng et al., 2023) and scientific literature (Zhang et al., 2026).

An analysis of the conservation of RBD mutations accumulated in predominant post-pandemic variants relative to the WT virus was performed using Grantham's distances (Grantham, 1974) according to a previously proposed classification (Li et al., 1984). Mutations with Grantham's distances of 0–50 were considered conservative, 51–100 moderately conservative, 101–150 moderately radical, and ≥151 radical (Li et al., 1984).

Subsequently, modeling of SARS-CoV-2 RBD complexes with the ACE2 receptor and a reference antibody (STE90-C11) was performed. The 6LZG structure (Wang et al., 2020) was used as the three-dimensional model for constructing complexes of RBDs with ACE2 (RBD-ACE2), whereas the 7B3O structure (Bertoglio et al., 2021) from the RCSB PDB was used for modeling complexes of RBDs with antibody (RBD-AB). Initially, RBD-ACE2 and RBD-AB complexes containing the WT RBD sequence were modeled using the SWISS-MODEL server (Waterhouse et al., 2018), together with intermediate templates containing the WT RBD sequence lacking the amino acid at position V483 to generate complexes characterized by the Δ483 deletion. Subsequently, mutations characteristic of the studied post-pandemic SARS-CoV-2 variants were introduced into the models containing either the WT RBD or the Δ483 modification using MODELLER 10.4 (Sali & Blundell, 1993).

To evaluate the effects of RBD mutations on affinity toward ACE2 and antibody, Gibbs binding free energy (ΔG) values were estimated. Calculations were performed using the Molecular Mechanics/Generalized Born Surface Area (MM/GBSA) method (Gohlke & Case, 2004) implemented in the HawkDock server v2 (Weng et al., 2019; Zhang et al., 2025). Changes in ΔG values were interpreted as indicators of altered affinity, where decreased ΔG values corresponded to increased affinity and increased ΔG values corresponded to decreased affinity. For ease of interpretation, the change in Gibbs binding free energy (ΔΔG) was additionally calculated according to the following equation:

$$\Delta\Delta G = \Delta G_{Mut} - \Delta G_{WT},$$

where ΔG_{WT} and ΔG_{Mut} represent the ΔG values for complexes containing the WT and mutated RBDs, respectively. Positive ΔΔG values indicated destabilization of the corresponding complex due to mutations, whereas negative ΔΔG values indicated stabilization.

Complexes with ACE2 and antibody containing the WT RBD, as well as the XBB.1.5 and BA.3.2.2 RBDs, were further analyzed using molecular dynamics simulations in GROMACS 2023.3 (Berendsen et al., 1995; Abraham et al., 2015). The CHARMM36m force field was applied (Huang et al., 2017). All studied systems, including both ACE2- and AB-containing complexes, were placed in a dodecahedral box with a minimum distance of 1.6 nm between the protein complex and the box edge, solvated, neutralized with NaCl, and adjusted to a salt concentration of 0.15 M, followed by energy minimization.

The equilibration procedure included the following stages: an NVT equilibration stage using the V-rescale thermostat (temperature coupling constant 0.1 ps) for 1 ns for all systems; a first NPT stage using the V-rescale thermostat (0.1 ps) and C-rescale barostat (pressure coupling constant 2.0 ps) for 1 ns; and a second NPT stage using the V-rescale thermostat (1.0 ps) and C-rescale barostat (5.0 ps) for 50 ns for ACE2-containing complexes or 100 ns for antibody-containing complexes. Production simulations were subsequently carried out for 200 ns for RBD-ACE2 complexes and 500 ns for RBD-AB complexes.

Primary trajectory analysis included calculation of the root mean square deviation (RMSD), root mean square fluctuation (RMSF), radius of gyration (Rg), solvent-accessible surface area (SASA) (Bondi, 1964; Eisenhaber et al., 1995), and the number of hydrogen bonds. Finally, ΔG values were estimated throughout the molecular dynamics trajectories using the Molecular Mechanics/Poisson-Boltzmann Surface Area (MM/PBSA) approach implemented in the gmx_MMPBSA package (Miller et al., 2012; Valdés-Tresanco et al., 2021).

In addition, principal component analysis (PCA) and free energy landscape (FEL) analysis were performed. For these analyses, trajectories corresponding to complexes of the same type (ACE2- and antibody-containing complexes analyzed separately) were fitted using backbone atoms and then concatenated (Cossio-Pérez et al., 2017). PCA was subsequently performed based on Cα atoms, and projections onto the first two principal eigenvectors were used to generate FEL heatmaps representing the Gibbs free energy (G, kJ/mol) distribution.

The open-source PyMOL program (Version 2.5, Schrödinger LLC, 2021) was used to visualize three-dimensional structures of the studied complexes.

Results

Table 1 presents the mutational profiles within the RBDs of post-pandemic SARS-CoV-2 variants designated as VOIs, as well as several variants classified as VUMs at the time of the study in 2026. The number of mutations within the RBD ranged from 21 in the BA.3.2.1 sublineage to 31 in the XFG variant. Each studied variant was characterized by a unique mutational profile within the RBD. However, several mutations were identified in all analyzed variants: S371F, S373P, S375F, D405N, R408S, K417N, N440K, N460K, S477N, Q498R, and N501Y. In addition, positions 339, 445, 446, 478, and 484 were altered in all variants relative to the WT virus, although the specific amino acid substitutions differed among variants. According to Grantham's distances, the identified mutations included substitutions from all four categories (conservative, moderately conservative, moderately radical, and radical), although moderately conservative and moderately radical substitutions predominated. Furthermore, several studied variants (BA.2.86, JN.1, KP.3.1.1, NB.1.8.1, and XFG) carried a deletion at position 483.

A visual representation of the three-dimensional structures of the RBD-ACE2 and RBD-AB complexes containing the WT RBD is presented in Figure 1. The figure also highlights the positions of mutations identified in one or more post-pandemic SARS-CoV-2 variants. As shown, the majority of these mutations are localized in close proximity to the binding interfaces of both the RBD-ACE2 and RBD-AB complexes.

Table 2 presents the estimated ΔG values for RBD-ACE2 and RBD-AB complexes formed by different SARS-CoV-2 variants, together with the corresponding ΔΔG values relative to the reference complexes formed by the WT virus RBD. As shown for the RBD-

ACE2 complexes, several studied SARS-CoV-2 variants formed more stable complexes with human ACE2 ($\Delta\Delta G < 0$) than the WT virus, including XBB.1.5, EG.5, BA.2.86, JN.1, and BA.3.2 sublineages (BA.3.2.1 and BA.3.2.2). Notably, the BA.3.2 sublineages demonstrated the highest affinity for the ACE2 receptor. The corresponding ΔG values for complexes formed by BA.3.2.1 and BA.3.2.2 were –74.56 and –73.16 kcal/mol, respectively, compared to –68.88 kcal/mol for the WT RBD-ACE2 complex. These findings indicate that these variants possess an increased affinity for ACE2 and therefore may interact with the human receptor more efficiently during the infectious process. In contrast, the RBDs of the remaining post-pandemic SARS-CoV-2 variants formed less stable complexes with ACE2 than the WT virus. Although the XBB.1.16 variant exhibited a ΔG value of –68.84 kcal/mol, which was nearly identical to the WT reference value, the XFG variant demonstrated substantially lower affinity for ACE2, with a ΔG value of –57.24 kcal/mol.

Table 1
Mutational profiles within the RBDs of post-pandemic SARS-CoV-2 variants

WT	Variants of concern (VOIs) during 2023–2026					Variants under monitoring (VUMs) in 2026				
	XBB.1.5	XBB.1.16	EG.5	BA.2.86	JN.1	KP.3.1.1	NB.1.8.1	XFG	BA.3.2	
									BA.3.2.1	BA.3.2.2
G339	H (98)	H (98)	H (98)	H (98)	H (98)	H (98)	H (98)	H (98)	Y (147)	Y (147)
R346	T (71)	T (71)	T (71)	—	—	—	—	T (71)	—	—
A348	—	—	—	—	—	—	—	—	P (27)	P (27)
K356	—	—	—	T (78)	T (78)	T (78)	T (78)	T (78)	—	T (78)
L368	I (5)	I (5)	I (5)	—	—	—	—	—	—	—
S371	F (155)	F (155)	F (155)	F (155)	F (155)	F (155)	F (155)	F (155)	F (155)	F (155)
S373	P (74)	P (74)	P (74)	P (74)	P (74)	P (74)	P (74)	P (74)	P (74)	P (74)
S375	F (155)	F (155)	F (155)	F (155)	F (155)	F (155)	F (155)	F (155)	F (155)	F (155)
T376	A (58)	A (58)	A (58)	A (58)	A (58)	A (58)	A (58)	A (58)	—	—
R403	—	—	—	K (26)	K (26)	K (26)	K (26)	K (26)	K (26)	K (26)
D405	N (23)	N (23)	N (23)	N (23)	N (23)	N (23)	N (23)	N (23)	N (23)	N (23)
R408	S (110)	S (110)	S (110)	S (110)	S (110)	S (110)	S (110)	S (110)	S (110)	S (110)
K417	N (94)	N (94)	N (94)	N (94)	N (94)	N (94)	N (94)	N (94)	N (94)	N (94)
A435	—	—	—	—	—	—	S (99)	—	S (99)	S (99)
N440	K (94)	K (94)	K (94)	K (94)	K (94)	K (94)	K (94)	K (94)	R (86)	R (86)
K444	—	—	—	—	—	—	—	R (26)	—	—
V445	P (68)	P (68)	P (68)	H (84)	H (84)	H (84)	H (84)	R (96)	A (64)	A (64)
G446	S (56)	S (56)	S (56)	S (56)	S (56)	S (56)	S (56)	S (56)	D (94)	D (94)
N450	—	—	—	D (23)	D (23)	D (23)	D (23)	D (23)	—	—
L452	—	—	—	W (61)	W (61)	W (61)	W (61)	W (61)	W (61)	W (61)
L455	—	—	—	—	S (145)	S (145)	S (145)	S (145)	—	—
F456	—	—	L (22)	—	—	L (22)	L (22)	L (22)	—	—
N460	K (94)	K (94)	K (94)	K (94)	K (94)	K (94)	K (94)	K (94)	K (94)	K (94)
S477	N (46)	N (46)	N (46)	N (46)	N (46)	N (46)	N (46)	N (46)	N (46)	N (46)
T478	K (78)	R (71)	K (78)	K (78)	K (78)	K (78)	I (89)	K (78)	N (65)	N (65)
N481	—	—	—	K (94)	K (94)	K (94)	K (94)	K (94)	—	—
V483	—	—	—	Δ	Δ	Δ	Δ	Δ	—	—
E484	A (107)	A (107)	A (107)	K (56)	K (56)	K (56)	K (56)	K (56)	K (56)	K (56)
F486	P (114)	P (114)	P (114)	P (114)	P (114)	P (114)	P (114)	P (114)	—	—
N487	—	—	—	—	—	—	—	D (23)	—	—
F490	S (155)	S (155)	S (155)	—	—	—	—	—	—	—
Q493	—	—	—	—	—	E (29)	E (29)	E (29)	—	—
G496	—	—	—	—	—	—	—	—	S (56)	S (56)
Q498	R (43)	R (43)	R (43)	R (43)	R (43)	R (43)	R (43)	R (43)	R (43)	R (43)
N501	Y (143)	Y (143)	Y (143)	Y (143)	Y (143)	Y (143)	Y (143)	Y (143)	Y (143)	Y (143)
Y505	H (83)	H (83)	H (83)	H (83)	H (83)	H (83)	H (83)	H (83)	—	—

Note: amino acids are presented using single-letter notation; positions within the S protein at which no mutations were detected in any studied variant relative to the WT virus are not shown in the table; Grantham's distances relative to the corresponding WT amino acids are indicated in parentheses next to each substituted residue. Substitutions with Grantham's distances of 0-50 were considered conservative, 51–100 moderately conservative, 101–150 moderately radical, and ≥151 radical.

Analysis of the RBD-AB complexes demonstrated that all studied post-pandemic variants exhibited reduced affinity for the antibody relative to the WT virus, forming less stable complexes. Consequently, the binding efficiency of antibodies to the RBDs of post-pandemic SARS-CoV-2 variants may be reduced compared to the WT virus. However, the magnitude of the ΔG and $\Delta\Delta G$ changes differed considerably among variants. For XBB.1.5, XBB.1.16, EG.5, and the BA.3.2 sublineages, $\Delta\Delta G$ values differed by approximately 20–30 kcal/mol relative to the reference ΔG value of –111.18 kcal/mol for the WT RBD-AB complex. Although these changes were substantial, even greater effects were observed for other variants. In particular, the XFG variant exhibited a $\Delta\Delta G$ value of 50.80 kcal/mol, indicating an almost twofold reduction in affinity for antibody relative to the WT reference complex. Therefore, although the XFG variant demonstrated reduced affinity for ACE2, which could theoretically impair receptor recognition, this effect may be partially compensated by markedly decreased affinity for antibody, potentially facilitating antibody evasion.

Overall, SARS-CoV-2 variants characterized by increased affinity for ACE2 exhibited less pronounced reductions in affinity for antibody than variants that simultaneously lost affinity for both ACE2 and antibody. A positive correlation was observed between the ΔG values of RBD-ACE2 and RBD-AB complexes formed by post-pandemic variants (Pearson correlation coefficient = 0.661, $P = 0.037$). Thus, increases in ΔG values for ACE2-containing complexes were accompanied by increases in ΔG values for antibody-containing complexes. In other words, mutational profiles associated with decreased affinity for antibody were also associated with reduced affinity for the ACE2 receptor.

Subsequently, molecular dynamics simulations were performed for complexes formed by the RBDs of the WT virus, XBB.1.5, and BA.3.2.2 variants with the ACE2 receptor and the STE90-C11 antibody. The results of the molecular dynamics trajectory analysis for the RBD-ACE2 complexes are presented in Figure 2. The RMSD plots (Fig. 2a) demonstrated gradual stabilization of structural fluctuations during the 200 ns simulations. The RMSF plots further showed that

fluctuations of both the RBDs of different viral variants (Fig. 2b) and the ACE2 receptor within the corresponding complexes (Fig. 2c) were generally similar across individual amino acid residues.

The mean Rg values (mean ± SD) for the RBD-ACE2 complexes were 3.21 ± 0.03, 3.19 ± 0.03, and 3.18 ± 0.03 nm for complexes containing the RBDs of the WT virus, XBB.1.5, and BA.3.2.2 variants, respectively, indicating overall similarity in conformational compactness (Fig. 2d). Similarly, the mean SASA values (mean ± SD) were 366.32 ± 4.24, 363.71 ± 4.29, and 361.03 ± 3.94 nm^2 for complexes containing the RBDs of the WT virus, XBB.1.5, and BA.3.2.2 variants, respectively, suggesting generally similar solvent accessibility and diffusivity characteristics (Fig. 2e).

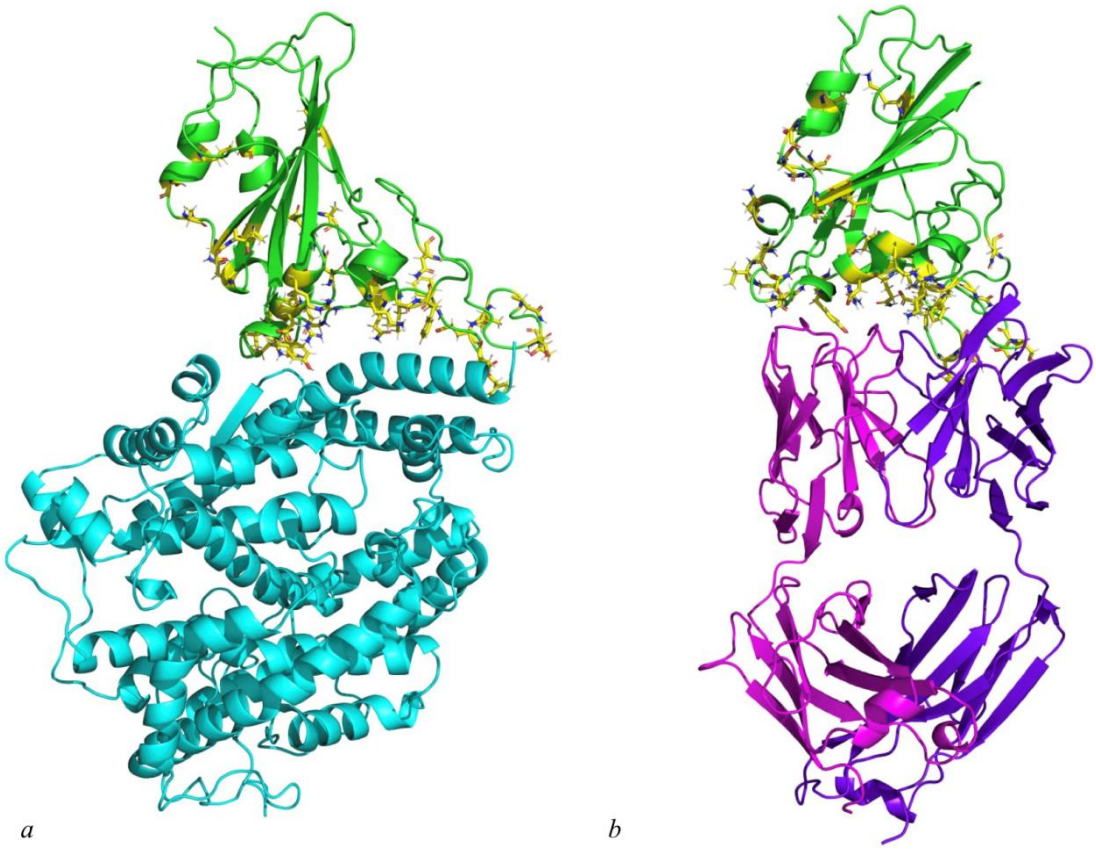

Fig. 1. Three-dimensional structures of RBD-ACE2 and RBD-AB complexes: *a* – structure of the WT RBD in complex with human ACE2; *b* – structure of the WT RBD in complex with the STE90-C11 antibody; the SARS-CoV-2 RBD is shown in green, the ACE2 receptor in cyan, and the heavy and light chains of the antibody in purple and magenta, respectively; RBD residues corresponding to mutation sites identified in the studied post-pandemic SARS-CoV-2 variants are highlighted in yellow using stick representation

Table 2
Binding free energies (ΔG) of RBD-ACE2 and RBD-AB complexes formed by different post-pandemic SARS-CoV-2 variants and corresponding changes (ΔΔG) relative to the WT virus, kcal/mol

SARS-CoV-2 variant	Complexes with ACE2		Complexes with antibody	
	ΔG	ΔΔG	ΔG	ΔΔG
WT	–68.88	—	–111.18	—
XBB.1.5	–71.07	–2.19*	–89.76	21.42*
XBB.1.16	–68.84	0.04	–90.10	21.08*
EG.5	–69.32	–0.44*	–87.50	23.68*
BA.2.86	–72.88	–4.00*	–75.81	35.37*
JN.1	–70.05	–1.17*	–73.41	37.77*
KP.3.1.1	–66.73	2.15	–66.94	44.24*
NB.1.8.1	–68.07	0.81	–68.48	42.70*
XFG	–57.24	11.64	–60.38	50.80*
BA.3.2.1	–74.56	–5.68*	–82.65	28.53*
BA.3.2.2	–73.16	–4.28*	–83.02	28.16*

Note: ΔΔG values marked with * correspond to variants exhibiting a potential adaptive advantage, namely ΔΔG < 0 (increased interaction stability) for RBD-ACE2 complexes and ΔΔG > 0 (decreased interaction stability) for RBD-AB complexes.

Nevertheless, some differences were observed in the interactions between the RBDs of different variants and the ACE2 receptor. Figure 2f illustrates the dynamics of hydrogen bond formation between RBD and ACE2. The mean numbers of hydrogen bonds (mean ± SD) were 6.27 ± 1.74, 4.94 ± 1.58, and 6.49 ± 1.53 for complexes containing the RBDs of the WT virus, XBB.1.5, and BA.3.2.2 variants, respectively. Thus, the complex containing the XBB.1.5 RBD formed fewer hydrogen bonds than complexes containing the WT or BA.3.2.2 RBDs.

At the same time, the binding affinity of the RBDs toward the ACE2 receptor during molecular dynamics simulations was evaluated based on total binding free energy (ΔG^{total}, Fig. 2g), as well as its major components, namely binding free energy in the gas phase (ΔG^{gas}, Fig. 2h) and solvation free energy ($\Delta G^{solvation}$, Fig. 2i). The average ΔG^{total} values (mean ± SD) were −42.71 ± 12.01 kcal/mol, −53.58 ± 12.25 kcal/mol, and −59.03 ± 11.59 kcal/mol for complexes containing the RBDs of the WT virus, XBB.1.5, and BA.3.2.2 variants, respectively. Therefore, both the XBB.1.5 and BA.3.2.2 variants exhibited higher affinity for the ACE2 receptor than the WT virus, as indicated by their more negative ΔG^{total} values.

Figure 3 presents the results of molecular dynamics trajectory analysis for the RBD-AB complexes. The RMSD plots (Fig. 3a) demonstrate gradual stabilization of complexes formed by the RBDs of the WT virus, XBB.1.5, and BA.3.2.2 variants with the reference antibody during the 500 ns simulations. Analysis of the RMSF plots for the RBDs within these complexes (Fig. 3b) revealed that amino acid residues in the RBDs of the XBB.1.5 and BA.3.2.2 variants exhibited greater fluctuations during molecular dynamics simulations than the RBD of the WT virus. Examination of the RMSF plots for the antibody heavy and light chains (Fig. 3c-d) further showed that the values corresponding to complex containing the BA.3.2.2 RBD were higher than those of the WT and XBB.1.5 complexes. This finding indicates that both the heavy and light chains of the antibody displayed altered

dynamics and greater flexibility in the complex with the BA.3.2.2 variant.

Regarding the Rg of the RBD-AB complexes (Fig. 3e), the mean values (mean ± SD) were 3.19 ± 0.02 nm, 3.19 ± 0.05 nm, and 3.27 ± 0.06 nm for complexes containing the RBDs of the WT virus, XBB.1.5, and BA.3.2.2 variants, respectively, indicating slightly lower compactness of the complex containing the RBD of the BA.3.2.2. Similarly, the mean SASA values (mean ± SD) were 290.41 ± 3.55, 289.81 ± 5.20, and 298.58 ± 5.02 nm^2 for complexes containing the RBDs of the WT virus, XBB.1.5, and BA.3.2.2 variants, respectively, suggesting greater solvent accessibility and diffusivity for the BA.3.2.2 complex (Fig. 3f).

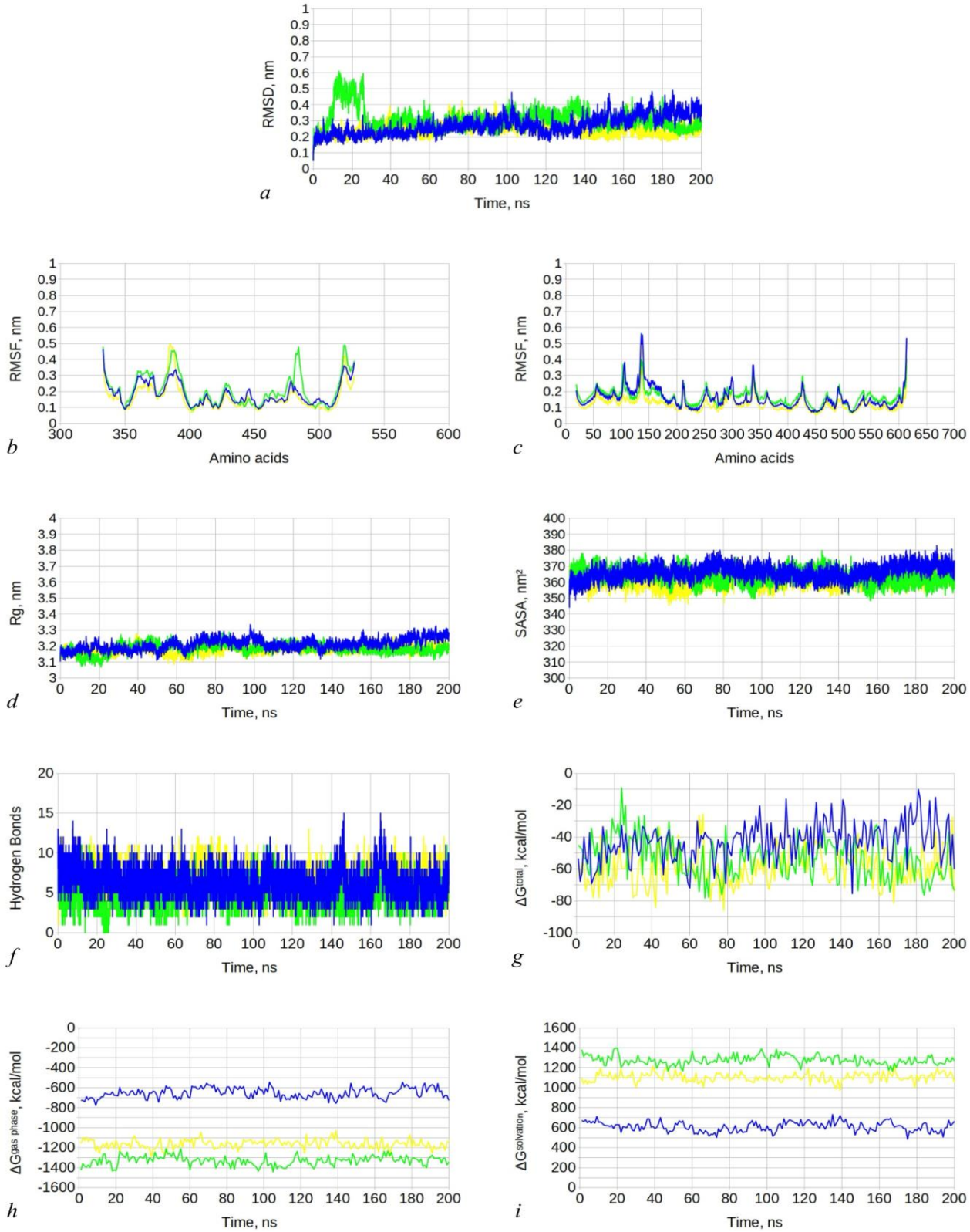

Fig. 2. Analysis of molecular dynamics trajectories of RBD-ACE2 complexes involving different SARS-CoV-2 variants: *a* – root mean square deviation (RMSD), *b* – root mean square fluctuation (RMSF) of SARS-CoV-2 RBDs, *c* – RMSF of human ACE2, *d* – radius of gyration (Rg), *e* – solvent-accessible surface area (SASA), *f* – number of hydrogen bonds between RBD and ACE2, *g* – total binding free energy (ΔG^{total}), *h* – binding free energy in the gas phase (ΔG^{gas}), *i* – solvation free energy ($\Delta G^{solvation}$); curves corresponding to complexes containing the WT RBD are shown in blue, XBB.1.5 in green, and BA.3.2.2 in yellow

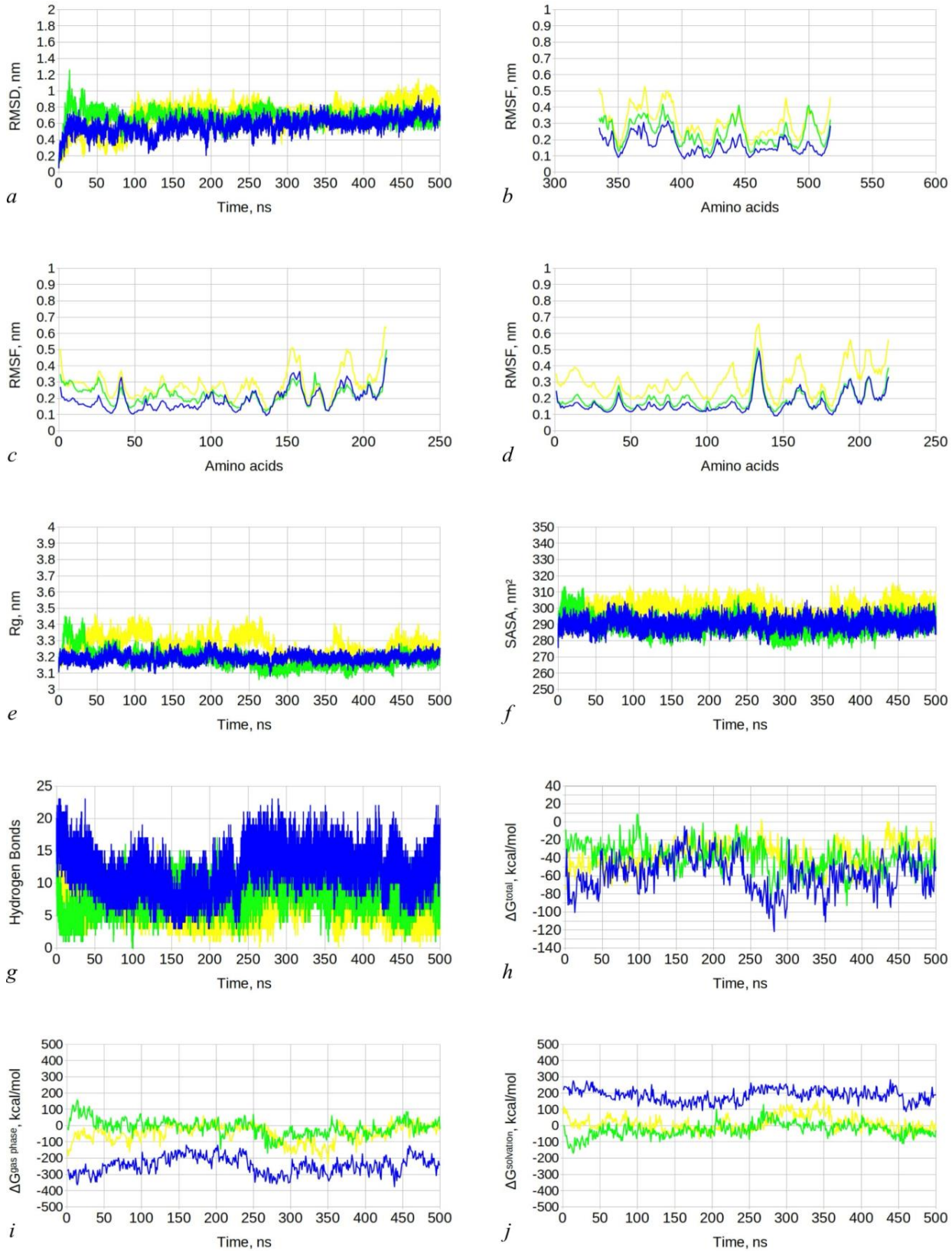

Fig. 3. Analysis of molecular dynamics trajectories of RBD-AB complexes involving different SARS-CoV-2 variants: *a* – root mean square deviation (RMSD), *b* – root mean square fluctuation (RMSF) of SARS-CoV-2 RBDs, *c* – RMSF of the heavy chain of the antibody, *d* – RMSF of the light chain of the antibody, *e* – radius of gyration (Rg), *f* – solvent-accessible surface area (SASA), *g* – number of hydrogen bonds between RBD and antibody, *h* – total binding free energy (ΔG^{total}), *i* – binding free energy in the gas phase (ΔG^{gas}), *j* – solvation free energy ($\Delta G^{solvation}$); curves corresponding to complexes containing the WT RBD are shown in blue, XBB.1.5 in green, and BA.3.2.2 in yellow

With respect to hydrogen bonding between RBD and antibody, the largest number of hydrogen bonds was observed for the complex containing the WT RBD (Fig. 3g). The mean numbers of hydrogen bonds (mean ± SD) during molecular dynamics simulations were 12.06 ± 3.19, 8.23 ± 2.46, and 6.82 ± 2.79 for complexes containing the RBDs of the WT virus, XBB.1.5, and BA.3.2.2 variants, respectively.

Figure 3h-j illustrate the dynamics of ΔG^{total}, ΔG^{gas}, and $\Delta G^{solvation}$ for the RBD-AB complexes. The average ΔG^{total} values were −58.14 ± 19.72 kcal/mol, −39.18 ± 16.12 kcal/mol, and −36.73 ±

14.59 kcal/mol for complexes containing the RBDs of the WT virus, XBB.1.5, and BA.3.2.2 variants, respectively. Therefore, both the XBB.1.5 and BA.3.2.2 variants exhibited reduced affinity for the reference antibody compared to the WT virus.

Figure 4 presents the results of PCA and FEL analysis. PCA projections onto the first two eigenvectors for the RBD-ACE2 complexes (Fig. 4a-d) accounted for 28.13% and 19.79% of the total structural variability observed during molecular dynamics simulations, respectively. The conformational spaces sampled by complexes containing RBDs of different SARS-CoV-2 variants partially overlapped (Fig. 4a). However, FEL analysis of the corresponding complexes (Fig. 4e-g) demonstrated that each complex was characterized by a distinct pattern of energy minima, indicating the acquisition of different dominant conformational states during molecular dynamics simulations. In particular, the complex containing the XBB.1.5 RBD exhibited several energy minima (Fig. 4f), one of which partially overlapped with the principal energy minimum observed for the BA.3.2.2 complex (Fig. 4g). In contrast, the dominant energy minimum of the WT RBD-ACE2 complex (Fig. 4e) differed substantially from those observed for the later SARS-CoV-2 variants.

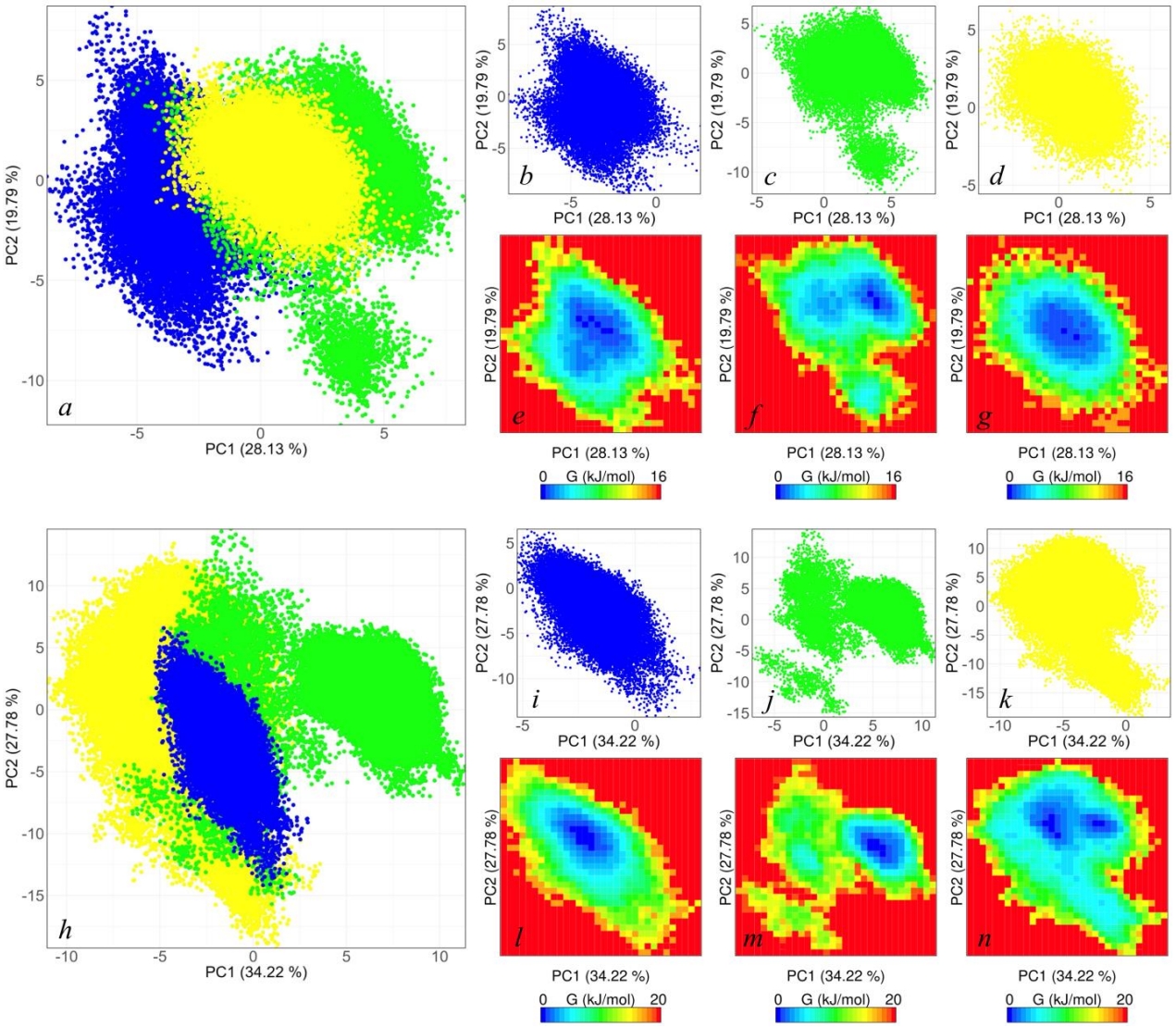

Fig 4. Principal component analysis (PCA) and free energy landscape (FEL) analysis based on molecular dynamics trajectories of RBD-ACE2 and RBD-AB complexes involving different SARS-CoV-2 variants: *a* – combined PCA projections for RBD-ACE2 complexes involving RBDs of different SARS-CoV-2 variants; *b* – PCA projection for the RBD-ACE2 complex containing the WT RBD; *c* – PCA projection for the RBD-ACE2 complex containing the XBB.1.5 RBD; *d* – PCA projection for the RBD-ACE2 complex containing the BA.3.2.2 RBD; *e* – FEL heatmap for the RBD-ACE2 complex containing the WT RBD; *f* – FEL heatmap for the RBD-ACE2 complex containing the XBB.1.5 RBD; *g* – FEL heatmap for the RBD-ACE2 complex containing the BA.3.2.2 RBD; *h* – combined PCA projections for RBD-AB complexes involving RBDs of different SARS-CoV-2 variants; *i* – PCA projection for the RBD-AB complex containing the WT RBD; *j* – PCA projection for the RBD-AB complex containing the XBB.1.5 RBD; *k* – PCA projection for the RBD-AB complex containing the BA.3.2.2 RBD; *l* – FEL heatmap for the RBD-AB complex containing the WT RBD; *m* – FEL heatmap for the RBD-AB complex containing the XBB.1.5 RBD; *n* – FEL heatmap for the RBD-AB complex containing the BA.3.2.2 RBD; on PCA plots, complexes containing the WT RBD are shown in blue, XBB.1.5 in green, and BA.3.2.2 in yellow

For the RBD-AB complexes, PCA projections onto the first two eigenvectors (Fig. 4h-k) accounted for 34.22% and 27.78% of the total structural variability, respectively. The conformational space sampled by the WT RBD-AB complex (Fig. 4i) was substantially smaller than those sampled by the XBB.1.5 (Fig. 4j) and BA.3.2.2 (Fig. 4k) complexes. This finding suggests that complexes containing the RBDs of XBB.1.5 and BA.3.2.2 transitioned through a larger number of metastable conformational states during molecular dynamics simulations, whereas the WT complex remained comparatively more stable. Similarly, FEL analysis (Fig. 4l-n) demonstrated that each RBD-AB complex possessed a distinct pattern of energy minima. These results indicate that the RBDs of different SARS-CoV-2 variants exhibit different conformational dynamics when interacting with the antibody.

Discussion

In this study, the interactions of several post-pandemic SARS-CoV-2 variants with the ACE2 receptor and antibody were analyzed. Both types of interactions are critical for successful viral spread. Variants that bind more efficiently to ACE2 may gain enhanced transmissibility, whereas variants that interact less efficiently with neutralizing antibodies may acquire advantages associated with immune evasion (Ataya et al., 2025; Alshahrani et al., 2026). Consequently, optimization of these properties may provide SARS-CoV-2 variants with substantial evolutionary advantages.

In this study, the STE90-C11 antibody (Bertoglio et al., 2021) was used as a reference antibody. This antibody was previously shown experimentally to effectively neutralize the WT virus and several early pandemic VOCs, including the Delta variant, but demonstrated markedly reduced neutralizing activity against the Omicron variant (Abassi et al., 2023). Because the post-pandemic variants analyzed in this study are descendants of Omicron lineages, STE90-C11 was expected to clearly demonstrate differences in binding between the WT RBD and the RBDs of later SARS-CoV-2 variants.

The calculated ΔG values for RBD-ACE2 and RBD-AB complexes formed by different post-pandemic SARS-CoV-2 variants demonstrated that all studied variants formed less stable complexes with the reference antibody than the WT virus. Only a subset of the variants formed more stable complexes with ACE2. The computational nature of all estimates obtained in this study imposes certain limitations on the interpretation of the results. However, these findings suggest that immune evasion may currently represent the predominant evolutionary direction of SARS-CoV-2 adaptation. Indeed, whereas the first Omicron lineages (BA.1, BA.2, BA.3, BA.4, and BA.5) contained approximately 30 mutations within the S protein, including 15–17 mutations in the RBD (Jawad et al., 2023; Peka & Balatsky, 2023), the variants analyzed in the present study carried 21–31 mutations within the RBD alone, in addition to numerous mutations in other regions of the S protein. The further accumulation of mutations within the same functional region likely complicates the simultaneous optimization of two competing properties: enhanced receptor binding and reduced antibody recognition. This is particularly important because host immune responses continue to evolve over time due to natural infection, vaccination, and updated vaccine formulations. Therefore, continuous adaptation to immune pressure remains an ongoing evolutionary requirement for emerging SARS-CoV-2 variants (Uzer et al., 2026).

XBB.1.5 (also known by the nickname “Kraken”) and XBB.1.16 (“Arcturus”) are descendants of the XBB lineage, which originated as a recombinant of two BA.2-derived Omicron sublineages (Planas et al., 2024; Zhang et al., 2024). XBB.1.5 was designated as a VOI by both the WHO and ECDC in January 2023 (Islam et al., 2023), whereas XBB.1.16 was classified as a VOI by the WHO in April 2023 and as a VUM by the ECDC in March 2023 (John et al., 2023; Looi, 2023). Both variants became prevalent during 2023 (Islam et al., 2023; Looi, 2023; Feng et al., 2024), and their mutational profiles contributed to both enhanced ACE2 binding and immune evasion (Sharma et al., 2023; Tamura et al., 2023; Yamasoba et al., 2023; Mannar et al., 2024). The ΔG calculations performed in the present study likewise identified XBB.1.5 as a variant characterized by both enhanced ACE2 binding and reduced affinity for the reference antibody. In contrast, XBB.1.16 demonstrated increased immune escape potential due to the formation of a less stable complex with the antibody, although no substantial advantage in ACE2 binding was observed.

The EG.5 variant (“Eris”), which also originated from the XBB lineage, possesses an RBD mutational profile similar to that of XBB.1.5 and was designated as a VOI by the WHO in August 2023 (Parums, 2023; da Costa et al., 2025). EG.5 became one of the dominant circulating variants during the second half of 2023 (Parums, 2023; Yadav et al., 2023). Compared with XBB.1.5, EG.5 carries an additional F456L mutation and has been suggested to possess enhanced immune evasion capacity (Sil et al., 2024; da Costa et al., 2025). Consistent with previous findings, the present ΔG analysis identified EG.5 as a variant capable of forming relatively stable complexes with ACE2 while simultaneously forming less stable complexes with the reference antibody compared to the WT virus. Moreover, EG.5 demonstrated a greater reduction in antibody affinity than either XBB.1.5 or XBB.1.16.

The BA.2.86 variant (“Pirola”) was designated as a VOI by both the WHO and ECDC in November 2023 (Spiess et al., 2024; Veneri et al., 2024). Subsequently, in December 2023, the WHO classified its descendant JN.1 as a separate VOI, which became widely disseminated during 2024 (Naveed Siddiqui et al., 2025; Traore et al., 2025). These variants are characterized by the presence of additional mutations relative to earlier XBB-derived lineages, with JN.1 carrying an additional L455S substitution compared to BA.2.86 (Naveed Siddiqui et al., 2025). Previous studies have suggested that BA.2.86 achieved a balance between efficient ACE2 binding and immune evasion (Yang et al., 2023; Liu et al., 2024a), whereas JN.1 exhibited even greater antibody escape capability (Naveed Siddiqui et al., 2025) but somewhat reduced ACE2 binding efficiency (Patterson et al., 2025) compared to BA.2.86. The present study likewise demonstrated that both BA.2.86 and JN.1 substantially reduced their affinity for the reference antibody, as well as increased affinity for ACE2 compared to WT virus, with BA.2.86 outperforming JN.1 in receptor binding efficiency, and JN.1, on the contrary, better evading the antibody than BA.2.86.

Several additional SARS-CoV-2 variants were classified as VUMs by the WHO during the post-pandemic period, including descendants of the JN.1 lineage such as KP.3.1.1, NB.1.8.1 (“Nimbus”), and XFG (“Stratus”), which retained this status in 2026 (Shi et al., 2025; Uriu et al., 2025; Azhar et al., 2026). Among these variants, KP.3.1.1 became widespread during 2024, whereas NB.1.8.1 and XFG circulated predominantly during the second half of 2025 (Cao et al., 2025; Shi et al., 2025). Similar to their predecessors, the mutational profiles of these variants contribute to enhanced immune evasion (Cao et al., 2025; Dadonaite et al., 2025; Guo et al., 2025). At the same time, the XFG variant accumulated as many as 31 mutations within the RBD, including the N487D substitution, which has been associated with substantially reduced affinity for ACE2 (Guo et al., 2025; Mellis et al., 2025). The marked reduction in affinity of the XFG variant for both the antibody and ACE2 observed in the present study is consistent with these previous findings.

One of the most recent variants to achieve substantial dissemination at the time of writing was BA.3.2 (including its sublineages BA.3.2.1 and BA.3.2.2) which was designated as VUM by the WHO in December 2025 and became widespread during 2026 (Fourati & Loubet, 2026; Shakya et., 2026). The BA.3.2 lineage has been suggested to possess greater immune evasion capacity than JN.1-derived variants (Guo et al., 2025), although it may exhibit lower ACE2 binding affinity relative to JN.1. However, the current findings suggest that BA.3.2 may possess a relatively balanced adaptive profile, combining enhanced ACE2 binding affinity compared with the WT virus and several later variants together with reduced antibody recognition.

Additional important findings of this study were obtained through molecular dynamics simulations of the RBD-ACE2 and RBD-AB complexes. Molecular dynamics analysis was performed for complexes containing the RBDs of the WT virus, the XBB.1.5 variant, which became widespread shortly after the end of the pandemic phase, and the BA.3.2.2 sublineage, which represented one of the most recently disseminated VUMs at the time of the study. The molecular dynamics results demonstrated the utility of *in silico* approaches for predicting the stability and binding properties of complexes containing SARS-CoV-2 RBDs. Specifically, the simulations showed that RBD-ACE2 and RBD-AB complexes may exhibit distinct conformational dynamics depending on the mutational profile of a given variant. These conformational differences were accompanied by changes in the number of hydrogen bonds, ΔG values, and overall complex stability.

The molecular dynamics results further indicated that post-pandemic variants such as XBB.1.5 and BA.3.2.2 bind the ACE2 receptor more efficiently than the WT virus. At the same time, complexes formed between these post-pandemic variants and the reference antibody

were conformationally less stable and exhibited weaker antibody binding than the complex involving the WT virus. In particular, the currently circulating BA.3.2.2 sublineage demonstrated both more efficient ACE2 binding and greater reduction in antibody interaction than the previously widespread XBB.1.5 variant.

Given that COVID-19 remains an important challenge for healthcare systems and that novel SARS-CoV-2 variants continue to emerge during the post-pandemic period (Verma et al., 2024; Saha et al., 2025), continuous monitoring of the biological properties of newly emerging variants remains essential for the timely prevention of both regional and global outbreaks (Uludağ et al., 2024). In this context, bioinformatic approaches provide effective tools for rapid screening and assessment of the effects of mutations and their combinations on the ability of SARS-CoV-2 to interact with cellular receptors and neutralizing antibodies.

Conclusions

The present study demonstrated that post-pandemic SARS-CoV-2 variants accumulated numerous mutations within the RBD of the S protein, resulting in altered interactions with both the ACE2 receptor and neutralizing antibodies. All studied variants formed less stable complexes with the reference antibody than the WT virus, indicating a general evolutionary trend toward immune evasion. However, only several variants exhibited enhanced affinity for ACE2, suggesting a trade-off between receptor binding optimization and antibody escape during viral evolution. Molecular dynamics simulations confirmed that mutations in post-pandemic variants substantially affect the conformational dynamics and stability of RBD-ACE2 and RBD-AB complexes. In particular, XBB.1.5 and BA.3.2.2 formed more stable complexes with ACE2 and less stable complexes with the reference antibody than the WT virus. PCA and FEL analyses further demonstrated mutation-associated differences in conformational landscapes and metastable states among the studied variants. Overall, the obtained results indicate that post-pandemic evolution of SARS-CoV-2 is primarily associated with adaptation toward immune evasion while maintaining sufficient ACE2 affinity for effective transmissibility. The performed analyses further demonstrate that integrated structural bioinformatics and molecular dynamics approaches can provide valuable insights into the adaptive potential of newly emerging SARS-CoV-2 lineages.

The authors declare no conflicts of interest.

References

Abassi, L., Bertoglio, F., Mačak Šafranko, Ž., Schirrmann, T., Greweling-Pils, M., Seifert, O., Khan, F., Katzmarzyk, M., Jacobsen, H., Gödecke, N., Heine, P. A., Frenzel, A., Nowack, H., Dübel, S., Kurolt, I. C., Kontermann, R. E., Markotić, A., Schubert, M., Hust, M., & Čičin-Šain, L. (2023). Evaluation of the neutralizing antibody STE90-C11 against SARS-CoV-2 Delta infection and its recognition of other variants of concerns. Viruses, 15(11), 2153.

Aboul-Fotouh, S., Mahmoud, A. N., Elnahas, E. M., Habib, M. Z., & Abdelraouf, S. M. (2023). What are the current anti-COVID-19 drugs? From traditional to smart molecular mechanisms. Virology Journal, 20(1), 241.

Abraham, M. J., Murtola, T., Schulz, R., Páll, S. Smith, J. C., Hess, B., & Lindahl, E. (2015). GROMACS: High performance molecular simulations through multi-level parallelism from laptops to supercomputers. SoftwareX, 1–2, 19–25.

Alhamlan, F. S., & Al-Qahtani, A. A. (2025). SARS-CoV-2 variants: Genetic insights, epidemiological tracking, and implications for vaccine strategies. International Journal of Molecular Sciences, 26(3), 1263.

Alshahrani, M., Gatlin, W., Ludwick, M., Turano, L., Foley, B., & Verkhivker, G. (2026). Mechanisms of binding and immune escape resistance for broadly neutralizing antibodies targeting distinct conserved SARS-CoV-2 spike epitopes: A hierarchical approach integrating mutational profiling and energy landscape analysis. International Journal of Molecular Sciences, 27(9), 4025.

Alves, M. C. S., da Silva, R. C. C., de Leitão-Júnior, S. S. P., & de Balbino, V. Q. (2025). Therapeutic approaches for COVID-19: a review of antiviral treatments, immunotherapies, and emerging interventions. Advances in Therapy, 42(7), 3045–3058.

Ambrosio, L., Chiara, M., Lo Presti, A., Poletti, P., Alteri, C., Cacchiarelli, D., Bouchè, V., Morgante, M., Ballabio, A., Perno, C. F., Merler, S., Pesole, G., & Stefanelli, P. (2022). SARS-CoV-2 variants: What have we learnt so far? Annali dell'Istituto Superiore Di Sanità, 58(2), 81–84.

Andre, M., Lau, L. S., Pokharel, M. D., Ramelow, J., Owens, F., Souchak, J., Akkaoui, J., Ales, E., Brown, H., Shil, R., Nazaire, V., Manevski, M., Paul, N. P., Esteban-Lopez, M., Ceyhan, Y., & El-Hage, N. (2023). From Alpha to Omicron: How different variants of concern of the SARS-Coronavirus-2 impacted the world. Biology, 12(9), 1267.

Ataya, F., Alamro, A., Alghamdi, A., & Fouad, D. (2025). SARS-CoV-2 spike mutations alter structure and energetics to modulate ACE2 binding immune evasion and viral adaptation. Scientific Reports, 15(1), 37546.

Ayenigbara I. O. (2020). COVID-19: An international public health concern. Central Asian Journal of Global Health, 9(1), e466.

Azhar, L. E., Samkari, D. A., Hassan, A. M., Alsayed, S. M., & Azhar, E. I. (2026). The emergence and characterization of SARS-CoV-2 variant XFG ("Stratus"): Comparative virological, epidemiological, and public-health perspectives. Journal of Epidemiology and Global Health, 16(1), 8.

Banerjee, S., Wang, X., Du, S., Zhu, C., Jia, Y., Wang, Y., & Cai, Q. (2022). Comprehensive role of SARS-CoV-2 spike glycoprotein in regulating host signaling pathway. Journal of Medical Virology, 94(9), 4071–4087.

Berendsen, H. J. C., van der Spoel, D., & van Drunen, R. (1995). GROMACS: A message-passing parallel molecular dynamics implementation. Computer Physics Communications, 91(1–3), 43–56.

Bertoglio, F., Fühner, V., Ruschig, M., Heine, P. A., Abassi, L., Klünemann, T., Rand, U., Meier, D., Langreder, N., Steinke, S., Ballmann, R., Schneider, K. T., Roth, K. D. R., Kuhn, P., Riese, P., Schäckermann, D., Korn, J., Koch, A., Chaudhry, M. Z., Eschke, K., … Hust, M. (2021). A SARS-CoV-2 neutralizing antibody selected from COVID-19 patients binds to the ACE2-RBD interface and is tolerant to most known RBD mutations. Cell Reports, 36(4), 109433.

Bocquet-Garçon, A. (2024). Impact of the SARS-CoV-2 spike protein on the innate immune system: A review. Cureus, 16(3), e57008.

Bondi, A. (1964). Van der Waals volumes and radii. Journal of Physical Chemistry, 68, 441–451.

Bourgonje, A. R., Abdulle, A. E., Timens, W., Hillebrands, J. L., Navis, G. J., Gordijn, S. J., Bolling, M. C., Dijkstra, G., Voors, A. A., Osterhaus, A. D., van der Voort, P. H., Mulder, D. J., & van Goor, H. (2020). Angiotensin-converting enzyme 2 (ACE2), SARS-CoV-2 and the pathophysiology of coronavirus disease 2019 (COVID-19). The Journal of Pathology, 251(3), 228–248.

Burki T. (2023). WHO ends the COVID-19 public health emergency. The Lancet. Respiratory Medicine, 11(7), 588.

Cao, G., Xu, C., Wang, L., Chai, K., & Wu, B. (2025). Global surveillance and biological characterization of the SARS-CoV-2 NB.1.8.1 variant: An emerging VUM lineage under scrutiny. Viruses, 17(11), 1457.

Carabelli, A. M., Peacock, T. P., Thorne, L. G., Harvey, W. T., Hughes, J., COVID-19 Genomics UK Consortium, Peacock, S. J., Barclay, W. S., de Silva, T. I., Towers, G. J., & Robertson, D. L. (2023). SARS-CoV-2 variant biology: Immune escape, transmission and fitness. Nature Reviews. Microbiology, 21(3), 162–177.

Chen, C., Nadeau, S., Yared, M., Voinov, P., Xie, N., Roemer, C., & Stadler, T. (2022). CoV-Spectrum: Analysis of globally shared SARS-CoV-2 data to identify and characterize new variants. Bioinformatics, 38(6), 1735–1737.

Chung, Y. S., Lam, C. Y., Tan, P. H., Tsang, H. F., & Wong, S. C. (2024). Comprehensive review of COVID-19: Epidemiology, pathogenesis, advancement in diagnostic and detection techniques, and post-pandemic treatment strategies. International Journal of Molecular Sciences, 25(15), 8155.

Cocherie, T., Zafilaza, K., Leducq, V., Marot, S., Calvez, V., Marcelin, A. G., & Todesco, E. (2022). Epidemiology and characteristics of SARS-CoV-2 variants of concern: The impacts of the spike mutations. Microorganisms, 11(1), 30.

Cossio-Pérez, R., Palma, J., & Pierdominici-Sottile, G. (2017). Consistent principal component modes from molecular dynamics simulations of proteins. Journal of Chemical Information and Modeling, 57(4), 826–834.

da Costa, C. H. S., de Freitas, C. A. B., Dos Santos, A. M., da Silva de Souza, C. G., Silva, J. R. A., Lameira, J., Moliner, V., & Skaf, M. S. (2025). Conformational dynamics and binding interactions of SARS-CoV-2 spike protein variants: Omicron, XBB.1.9.2, and EG.5. Journal of Chemical Information and Modeling, 65(14), 7651–7667.

Dadonaite, B., Harari, S., Larsen, B. B., Kampman, L., Harteloo, A., Elias-Warren, A., Chu, H. Y., & Bloom, J. D. (2025). Spike mutations that affect the function and antigenicity of recent KP.3.1.1-like SARS-CoV-2 variants. Journal of Virology, 99(11), e0142325.

Eisenhaber, F., Lijnzaad, P., Argos, P., Sander, C. & Scharf, M. (1995). The double cubic lattice method: Efficient approaches to numerical integration of surface area and volume and to dot surface contouring of molecular assemblies. Journal of Computational Chemistry, 16, 273–284.

Faraji, N., Zeinali, T., Joukar, F., Aleali, M. S., Eslami, N., Shenagari, M., & Mansour-Ghanaei, F. (2024). Mutational dynamics of SARS-CoV-2: Impact on future COVID-19 vaccine strategies. Heliyon, 10(9), e30208.
Feng, Y., Su, Q., Li, L., He, X., Niu, P., Guo, X., Zhao, X., Tang, J., Jia, Z., Wang, J., Wu, C., Xia, B., Chen, Z., Wu, Y., Yang, J., Chen, S., Chen, C., Wang, S., & Dong, X. (2024). Genomic surveillance for SARS-CoV-2 variants: Dominance of XBB replacement – China, January–June 2023. China CDC Weekly, 6(15), 324–331.
Fourati, S., & Loubet, P. (2026). SARS-CoV-2 BA.3.2: Epidemiological trends and implications for prophylactic antibodies. New Microbes and New Infections, 70, 101727.
Gangavarapu, K., Latif, A. A., Mullen, J. L., Alkuzweny, M., Hufbauer, E., Tsueng, G., Haag, E., Zeller, M., Aceves, C. M., Zaiets, K., Cano, M., Zhou, X., Qian, Z., Sattler, R., Matteson, N. L., Levy, J. I., Lee, R. T. C., Freitas, L., Maurer-Stroh, S., GISAID Core and Curation Team, … Hughes, L. D. (2023). Outbreak.info genomic reports: Scalable and dynamic surveillance of SARS-CoV-2 variants and mutations. Nature Methods, 20(4), 512–522.
Gohlke, H., & Case, D. A. (2004). Converging free energy estimates: MM-PB(GB)SA studies on the protein-protein complex Ras-Raf. Journal of Computational Chemistry, 25(2), 238–250.
Grantham, R. (1974). Amino acid difference formula to help explain protein evolution. Science, 185(4154), 862–864.
Guan, X., Yang, Y., & Du, L. (2023). Advances in SARS-CoV-2 receptor-binding domain-based COVID-19 vaccines. Expert Review of Vaccines, 22(1), 422–439.
Guo, C., Yu, Y., Liu, J., Jian, F., Yang, S., Song, W., Yu, L., Shao, F., & Cao, Y. (2025). Antigenic and virological characteristics of SARS-CoV-2 variants BA.3.2, XFG, and NB.1.8.1. The Lancet. Infectious Diseases, 25(7), e374–e377.
Huang, J., Rauscher, S., Nawrocki, G., Ran, T., Feig, M., de Groot, B. L., Grubmüller, H., & MacKerell Jr., A. D. (2017). CHARMM36m: An improved force field for folded and intrinsically disordered proteins. Nature Methods, 14(1), 71–73.
Huang, Y., Yang, C., Xu, X. F., Xu, W., & Liu, S. W. (2020). Structural and functional properties of SARS-CoV-2 spike protein: Potential antivirus drug development for COVID-19. Acta Pharmacologica Sinica, 41(9), 1141–1149.
Hwang, Y. C., Lu, R. M., Su, S. C., Chiang, P. Y., Ko, S. H., Ke, F. Y., Liang, K. H., Hsieh, T. Y., & Wu, H. C. (2022). Monoclonal antibodies for COVID-19 therapy and SARS-CoV-2 detection. Journal of Biomedical Science, 29, 1.
Islam M. A. (2023). A review of SARS-CoV-2 variants and vaccines: Viral properties, mutations, vaccine efficacy, and safety. Infectious Medicine, 2(4), 247–261.
Islam, M. A., Kaifa, F. H., Chandran, D., Bhattacharya, M., Chakraborty, C., Bhattacharya, P., & Dhama, K. (2023). XBB.1.5: a new threatening SARS-CoV-2 Omicron subvariant. Frontiers in Microbiology, 14, 1154296.
Jawad, B., Adhikari, P., Podgornik, R., & Ching, W. Y. (2023). Impact of BA.1, BA.2, and BA.4/BA.5 Omicron mutations on therapeutic monoclonal antibodies. Computers in Biology and Medicine, 167, 107576.
John, O. O., Olabode, O. N., Lucero-Prisno Iii, D. E., Adebimpe, O. T., & Singh, A. (2023). XBB.1.16 Omicron subvariant rise to a variant of interest: Implications for global alertness and preparedness. Journal of Taibah University Medical Sciences, 18(6), 1285–1287.
Kung, Y. A., Chuang, C. H., Chen, Y. C., Yang, H. P., Li, H. C., Chen, C. L., Janapatla, R. P., Chen, C. J., Shih, S. R., & Chiu, C. H. (2025). Worldwide SARS-CoV-2 Omicron variant infection: Emerging sub-variants and future vaccination perspectives. Journal of the Formosan Medical Association, 124(7), 592–599.
Li, W. H., Wu, C. I., & Luo, C. C. (1984). Nonrandomness of point mutation as reflected in nucleotide substitutions in pseudogenes and its evolutionary implications. Journal of Molecular Evolution, 21(1), 58–71.
Liu, C., Zhou, D., Dijokaite-Guraliuc, A., Supasa, P., Duyvesteyn, H. M. E., Ginn, H. M., Selvaraj, M., Mentzer, A. J., Das, R., de Silva, T. I., Ritter, T. G., Plowright, M., Newman, T. A. H., Stafford, L., Kronsteiner, B., Temperton, N., Lui, Y., Fellermeyer, M., Goulder, P., Klenerman, P., … Screaton, G. R. (2024a). A structure-function analysis shows SARS-CoV-2 BA.2.86 balances antibody escape and ACE2 affinity. Cell Reports. Medicine, 5(5), 101553.
Liu, W., Huang, Z., Xiao, J., Wu, Y., Xia, N., & Yuan, Q. (2024b). Evolution of the SARS-CoV-2 Omicron variants: Genetic impact on viral fitness. Viruses, 16(2), 184.
Looi M. K. (2023). What do we know about the Arcturus XBB.1.16 subvariant? British Medical Journal, 381, 1074.
Lu, Y., Shen, F., He, W., Li, A., Li, M., Feng, X., Zheng, Y., & Pang, W. (2023). HR121 targeting HR2 domain in S2 subunit of spike protein can serve as a broad-spectrum SARS-CoV-2 inhibitor via intranasal administration. Acta Pharmaceutica Sinica, B, 13(8), 3339–3351.
Magazine, N., Zhang, T., Bungwon, A. D., McGee, M. C., Wu, Y., Veggiani, G., & Huang, W. (2024). Immune epitopes of SARS-CoV-2 spike protein and considerations for universal vaccine development. ImmunoHorizons, 8(3), 214–226.
Mannar, D., Saville, J. W., Poloni, C., Zhu, X., Bezeruk, A., Tidey, K., Ahmed, S., Tuttle, K. S., Vahdatihassani, F., Cholak, S., Cook, L., Steiner, T. S., & Subramaniam, S. (2024). Altered receptor binding, antibody evasion and retention of T cell recognition by the SARS-CoV-2 XBB.1.5 spike protein. Nature Communications, 15(1), 1854.
Markov, P. V., Ghafari, M., Beer, M., Lythgoe, K., Simmonds, P., Stilianakis, N. I., & Katzourakis, A. (2023). The evolution of SARS-CoV-2. Nature Reviews. Microbiology, 21(6), 361–379.
Mellis, I. A., Wu, M., Hong, H., Tzang, C. C., Bowen, A., Wang, Q., Gherasim, C., Pierce, V. M., Shah, J. G., Purpura, L. J., Yin, M. T., Gordon, A., Guo, Y., & Ho, D. D. (2025). Antibody evasion and receptor binding of SARS-CoV-2 LP.8.1.1, NB.1.8.1, XFG, and related subvariants. Cell Reports, 44(10), 116440.
Mengist, H. M., Kombe Kombe, A. J., Mekonnen, D., Abebaw, A., Getachew, M., & Jin, T. (2021). Mutations of SARS-CoV-2 spike protein: Implications on immune evasion and vaccine-induced immunity. Seminars in Immunology, 55, 101533.
Miller, B. R., 3rd, McGee Jr., T. D., Swails, J. M., Homeyer, N., Gohlke, H., & Roitberg, A. E. (2012). MMPBSA.py: An efficient program for end-state free energy calculations. Journal of Chemical Theory and Computation, 8(9), 3314–3321.
Murmu, N., Sarkar, M., Dey, S., Manna, R., Roy, S., Mondal, T., Halder, S., Bhattacharjee, N., Dash, S. K., & Giri, B. (2024). Efficacy and limitations of repurposed drugs and vaccines for COVID-19. Journal of Medicine, Surgery, and Public Health, 2, 100041.
Naveed Siddiqui, A., Musharaf, I., & Gulumbe, B. H. (2025). The JN.1 variant of COVID-19: Immune evasion, transmissibility, and implications for global health. Therapeutic Advances in Infectious Disease, 12, 20499361251314763.
Naveed, N., Ahmad, K., Majeed, H., Qureshi, K., Ahmad, I., Awan, M. F., Iftikhar, T., Ahmad, S., Noreen, F., Amin, M. A., & Batool, H. (2024). The global impact of COVID-19: A comprehensive analysis of its effects on various aspects of life. Toxicology Research, 13(2), tfae045.
Ou, X., Liu, Y., Lei, X., Li, P., Mi, D., Ren, L., Guo, L., Guo, R., Chen, T., Hu, J., Xiang, Z., Mu, Z., Chen, X., Chen, J., Hu, K., Jin, Q., Wang, J., & Qian, Z. (2020). Characterization of spike glycoprotein of SARS-CoV-2 on virus entry and its immune cross-reactivity with SARS-CoV. Nature Communications, 11(1), 1620.
Pak, A., Adegboye, O. A., Adekunle, A. I., Rahman, K. M., McBryde, E. S., & Eisen, D. P. (2020). Economic consequences of the COVID-19 outbreak: The need for epidemic preparedness. Frontiers in Public Health, 8, 241.
Pal, M., Berhanu, G., Desalegn, C., & Kandi, V. (2020). Severe acute respiratory syndrome coronavirus-2 (SARS-CoV-2): An update. Cureus, 12(3), e7423.
Parsons, R. J., & Acharya, P. (2023). Evolution of the SARS-CoV-2 Omicron spike. Cell Reports, 42(12), 113444.
Parums, D. V. (2023). Editorial: A rapid global increase in COVID-19 is due to the emergence of the EG.5 (Eris) subvariant of Omicron SARS-CoV-2. Medical Science Monitor, 29, e942244.
Patterson, L. D., Elsharkawy, A., Jahantigh, H. R., Nabi, Z., Stone, S., & Kumar, M. (2025). Pathogenicity of SARS-CoV-2 Omicron subvariants JN.1, KP.2, and EG.5.1 in K18-hACE2 transgenic mice. Viruses, 17(9), 1177.
Peka, M., & Balatsky, V. (2023). The impact of mutation sets in receptor-binding domain of SARS-CoV-2 variants on the stability of RBD-ACE2 complex. Future Virology, 18(4), 225–242.
Planas, D., Staropoli, I., Michel, V., Lemoine, F., Donati, F., Prot, M., Porrot, F., Guivel-Benhassine, F., Jeyarajah, B., Brisebarre, A., Dehan, O., Avon, L., Bolland, W. H., Hubert, M., Buchrieser, J., Vanhoucke, T., Rosenbaum, P., Veyer, D., Péré, H., Lina, B., … Schwartz, O. (2024). Distinct evolution of SARS-CoV-2 Omicron XBB and BA.2.86/JN.1 lineages combining increased fitness and antibody evasion. Nature Communications, 15(1), 2254.
Pourriyahi, H., Hajizadeh, N., Khosravi, M., Pourriahi, H., Soleimani, S., Hosseini, N. S., Mohammad, A. P., & Goodarzi, A. (2024). New variants of COVID-19 (XBB.1.5 and XBB.1.16, the "Arcturus"): A review of highly questioned concerns, a brief comparison between different peaks in the COVID-19 pandemic, with a focused systematic review on expert recommendations for prevention, vaccination, and treatment measures in the general population and at-risk groups. Immunity, Inflammation and Disease, 12(6), e1323.
Rabaan, A. A., Alenazy, M. F., Alshehri, A. A., Alshahrani, M. A., Al-Subaie, M. F., Alrasheed, H. A., Al Kaabi, N. A., Thakur, N., Bouafia, N. A., Alissa, M., Alsulaiman, A. M., AlBaadani, A. M., Alhani, H. M., Alhaddad,

A. H., Alfouzan, W. A., Ali, B. M. A., Al-Abdulali, K. H., Khamis, F., Bayahya, A., Al Fares, M. A., … Dhawan, M. (2023). An updated review on pathogenic coronaviruses (CoVs) amid the emergence of SARS-CoV-2 variants: A look into the repercussions and possible solutions. Journal of Infection and Public Health, 16(11), 1870–1883.

Rathore, J. S., & Ghosh, C. (2020). Severe acute respiratory syndrome coronavirus-2 (SARS-CoV-2), a newly emerged pathogen: An overview. Pathogens and Disease, 78(6), ftaa042.

Saadi, F., Pal, D., & Sarma, J. D. (2021). Spike glycoprotein is central to coronavirus pathogenesis-parallel between m-CoV and SARS-CoV-2. Annals of Neurosciences, 28(3–4), 201–218.

Saha, A., Ghosh Roy, S., Dwivedi, R., Tripathi, P., Kumar, K., Nambiar, S. M., & Pathak, R. (2025). Beyond the pandemic era: Recent advances and efficacy of SARS-CoV-2 vaccines against emerging variants of concern. Vaccines, 13(4), 424.

Saladino, V., Algeri, D., & Auriemma, V. (2020). The psychological and social impact of Covid-19: New perspectives of well-being. Frontiers in Psychology, 11, 577684.

Sali, A., & Blundell, T. L. (1993). Comparative protein modelling by satisfaction of spatial restraints. Journal of Molecular Biology, 234(3), 779–815.

Santo, K., Favaro, L., & Martins, E. (2025). Following the pandemic: Exploring long COVID's impact on global health through the World Heart Federation Global COVID-19 Study. Global Heart, 20(1), 79.

Sarker, R., Roknuzzaman, A. S. M., Hossain, M. J., Bhuiyan, M. A., & Islam, M. R. (2023). The WHO declares COVID-19 is no longer a public health emergency of international concern: benefits, challenges, and necessary precautions to come back to normal life. International Journal of Surgery, 109(9), 2851–2852.

Shakya, M., Ma, K. C., Hughes, L. J., Boehm, A. B., Cook, P. W., Cornforth, D. M., Gardner, M., Goraichuk, I. V., Harcourt, J. L., Hicks, H., Johnson, M., Kelleher, A., Reese, H. E., Sabin, S. J., Smith, T. C., Tamin, A., Wolfe, M. K., Silk, B. J., Paden, C. R., … MacNeil, A. (2026). Early detection and surveillance of the SARS-CoV-2 variant BA.3.2 – worldwide, November 2024–February 2026. MMWR and Morbidity and Mortality Weekly Report, 75, 130–137.

Sharma, T., Gerstman, B., & Chapagain, P. (2023). Distinctive features of the XBB.1.5 and XBB.1.16 spike protein receptor-binding domains and their roles in conformational changes and angiotensin-converting enzyme 2 binding. International Journal of Molecular Sciences, 24(16), 12586.

Shi, J., Zhao, X., Jin, X., Li, J., Liu, Y., Liu, H., Hu, Y. F., Chen, Z., Xiao, Y., Wang, L., Wang, Y., He, Y., Chai, Y., Hu, B., Shuai, H., Wang, Y., Li, X., Jiang, S., Zhang, Y., Zhang, X., … Chu, H. (2025). Pathogenicity, virological features, and immune evasion of SARS-CoV-2 JN.1-derived variants including JN.1.7, KP.2, KP.3, and KP.3.1.1. Nature Communications, 16(1), 11002.

Sil, D., Gautam, S., Saxena, S., Joshi, S., Kumar, D., Mehta, A., Jindal, P., Sharma, S., Pandey, P., Diksha, & Singh, A. (2024). Comprehensive analysis of Omicron subvariants: EG.5 rise, vaccination strategies, and global impact. Current Drug Targets, 25(8), 517–525.

Soares, V. C., Moreira, I. B. G., & Dias, S. S. G. (2025). SARS-CoV-2 infection and antiviral strategies: Advances and limitations. Viruses, 17(8), 1064.

Souza, U. J. B., Spilki, F. R., Tanuri, A., Roehe, P. M., & Campos, F. S. (2025). Two years of SARS-CoV-2 Omicron genomic evolution in Brazil (2022–2024): Subvariant tracking and assessment of regional sequencing efforts. Viruses, 17(1), 64.

Spiess, K., Petrillo, M., Paracchini, V., Leoni, G., Lassaunière, R., Polacek, C., Marving, E. L., Larsen, N. B., Gunalan, V., Ring, A., Bull, M., Buttinger, G., Veneri, C., Suffredini, E., La Rosa, G., Corbisier, P., Querci, M., Rasmussen, M., & Marchini, A. (2024). Development of new RT-PCR assays for the specific detection of BA.2.86 SARS-CoV-2 and its descendent sublineages. The Science of the Total Environment, 954, 176365.

Sun, M., Yan, S., Cao, T., & Zhang, J. (2024). The impact of COVID-19 pandemic on the world's major economies: based on a multi-country and multi-sector CGE model. Frontiers in Public Health, 12, 1338677.

Tamura, T., Ito, J., Uriu, K., Zahradnik, J., Kida, I., Anraku, Y., Nasser, H., Shofa, M., Oda, Y., Lytras, S., Nao, N., Itakura, Y., Deguchi, S., Suzuki, R., Wang, L., Begum, M. M., Kita, S., Yajima, H., Sasaki, J., Sasaki-Tabata, K., … Sato, K. (2023). Virological characteristics of the SARS-CoV-2 XBB variant derived from recombination of two Omicron subvariants. Nature Communications, 14(1), 2800.

Tradigo, G., Das, J. K., Vizza, P., Roy, S., Guzzi, P. H., & Veltri, P. (2023). Strategies and trends in COVID-19 vaccination delivery: What we learn and what we may use for the future. Vaccines, 11(9), 1496.

Traore, A., Charniga, K., Grellet, S., Terpant, G., Da Cruz, H., Lamy, A., Thomas, N., Gbaguidi, G., Mercier, A., Prudhomme, J., Visseaux, B., Vieillefond, V., Haim-Boukobza, S., Giannoli, J. M., RELAB Study Group, Laboratory group, Castro-Alvarez, J., Kouamen, A. C., Rameix-Welti, M. A., Beirrera-Ibraim, S., … Members of the RELAB Study Group (2025). Monitoring SARS-CoV-2 variants with complementary surveillance systems: risk evaluation of the Omicron JN.1 variant in France, August 2023 to January 2024. Euro Surveillance: Bulletin Europeen sur les Maladies Transmissibles, 30(1), 2400293.

Tsueng, G., Mullen, J. L., Alkuzweny, M., Cano, M., Rush, B., Haag, E., Lin, J., Welzel, D. J., Zhou, X., Qian, Z., Latif, A. A., Hufbauer, E., Zeller, M., Andersen, K. G., Wu, C., Su, A. I., Gangavarapu, K., & Hughes, L. D. (2023). Outbreak.info Research Library: A standardized, searchable platform to discover and explore COVID-19 resources. Nature Methods, 20(4), 536–540.

Uludağ, M., Incitti, R., Gao, X., Heeney, J. L., Gojobori, T., & Alam, I. (2024). Global surveillance of emerging SARS-CoV-2 variants. Bulletin of the World Health Organization, 102(6), 374–374A.

Uraki, R., Korber, B., Diamond, M. S., & Kawaoka, Y. (2026). SARS-CoV-2 variants: Biology, pathogenicity, immunity and control. Nature Reviews, Microbiology, 24(1), 8–28.

Uriu, K., Okumura, K., Uwamino, Y., Chen, L., Tolentino, J. E., Asakura, H., Nagashima, M., Sadamasu, K., Yoshimura, K., Ito, J., Sato, K., & Genotype to Phenotype Japan (G2P-Japan) Consortium (2025). Virological characteristics of the SARS-CoV-2 NB.1.8.1 variant. The Lancet. Infectious Diseases, 25(8), e443.

Uzer, F., Erendor, F., & Sanlioglu, S. (2026). SARS-CoV-2 variants and immune evasion: Mapping the future of vaccine design. Reviews in Medical Virology, 36(3), e70157.

Valdés-Tresanco, M. S., Valdés-Tresanco, M. E., Valiente, P. A., & Moreno, E. (2021). gmx_MMPBSA: A new tool to perform end-state free energy calculations with GROMACS. Journal of Chemical Theory and Computation, 17(10), 6281–6291.

Veneri, C., Brandtner, D., Mancini, P., Bonanno Ferraro, G., Iaconelli, M., Suffredini, E., Petrillo, M., Leoni, G., Paracchini, V., Gawlik, B. M., Marchini, A., SARI Network, & La Rosa, G. (2024). Tracking the spread of the BA.2.86 lineage in Italy through wastewater analysis. Food and Environmental Virology, 16(4), 449–457.

Verma, A., Manojkumar, A., Dhasmana, A., Tripathi, M. K., Jaggi, M., Chauhan, S. C., Chauhan, D. S., & Yallapu, M. M. (2024). Recurring SARS-CoV-2 variants: An update on post-pandemic, co-infections and immune response. Nanotheranostics, 8(2), 247–269.

Walls, A. C., Park, Y. J., Tortorici, M. A., Wall, A., McGuire, A. T., & Veesler, D. (2020). Structure, function, and antigenicity of the SARS-CoV-2 spike glycoprotein. Cell, 181(2), 281–292.e6.

Wang, Q., Zhang, Y., Wu, L., Niu, S., Song, C., Zhang, Z., Lu, G., Qiao, C., Hu, Y., Yuen, K. Y., Wang, Q., Zhou, H., Yan, J., & Qi, J. (2020). Structural and functional basis of SARS-CoV-2 entry by using human ACE2. Cell, 181(4), 894–904.e9.

Wang, X., Lu, L., & Jiang, S. (2023). SARS-CoV-2 Omicron subvariant BA.2.86: Limited potential for global spread. Signal Transduction and Targeted Therapy, 8(1), 439.

Waterhouse, A., Bertoni, M., Bienert, S., Studer, G., Tauriello, G., Gumienny, R., Heer, F. T., de Beer, T. A. P., Rempfer, C., Bordoli, L., Lepore, R., & Schwede, T. (2018). SWISS-MODEL: Homology modelling of protein structures and complexes. Nucleic Acids Research, 46(W1), W296–W303.

Weng, G., Wang, E., Wang, Z., Liu, H., Zhu, F., Li, D., & Hou, T. (2019). HawkDock: A web server to predict and analyze the protein-protein complex based on computational docking and MM/GBSA. Nucleic Acids Research, 47(W1), W322–W330.

Yadav, S., Zaman, K., Bashyal, P., Bhatta, R., Bhandari, S., Mohanty, A., & Sah, R. (2023). Newer emerging SARS-COV2 variant: Omicron EG.5. Annals of Medicine and Surgery (2012), 85(12), 5845–5846.

Yaghoubi, A., Amel Jamehdar, S., Movaqar, A., Milani, N., & Soleimanpour, S. (2021). An effective drug against COVID-19: reality or dream? Expert Review of Respiratory Medicine, 15(4), 505–518.

Yamasoba, D., Uriu, K., Plianchaisuk, A., Kosugi, Y., Pan, L., Zahradnik, J., Genotype to Phenotype Japan (G2P-Japan) Consortium, Ito, J., & Sato, K. (2023). Virological characteristics of the SARS-CoV-2 omicron XBB.1.16 variant. The Lancet. Infectious Diseases, 23(6), 655–656.

Yang, S., Yu, Y., Jian, F., Song, W., Yisimayi, A., Chen, X., Xu, Y., Wang, P., Wang, J., Yu, L., Niu, X., Wang, J., Xiao, T., An, R., Wang, Y., Gu, Q., Shao, F., Jin, R., Shen, Z., Wang, Y., … Cao, Y. (2023). Antigenicity and infectivity characterisation of SARS-CoV-2 BA.2.86. The Lancet, Infectious Diseases, 23(11), e457–e459.

Yang, S., Yu, Y., Xu, Y., Jian, F., Song, W., Yisimayi, A., Wang, P., Wang, J., Liu, J., Yu, L., Niu, X., Wang, J., Wang, Y., Shao, F., Jin, R., Wang, Y., & Cao, Y. (2024). Fast evolution of SARS-CoV-2 BA.2.86 to JN.1 under heavy immune pressure. The Lancet. Infectious Diseases, 24(2), e70–e72.

Zabidi, N. Z., Liew, H. L., Farouk, I. A., Puniyamurti, A., Yip, A. J. W., Wijesinghe, V. N., Low, Z. Y., Tang, J. W., Chow, V. T. K., & Lal, S. K. (2023). Evolution of SARS-CoV-2 variants: implications on immune escape, vaccination, therapeutic and diagnostic strategies. Viruses, 15(4), 944.

Zhang, L., Chen, N., Eichmann, A., Nehlmeier, I., Moldenhauer, A. S., Stankov, M. V., Happle, C., Dopfer-Jablonka, A., Behrens, G. M. N., Hoffmann, M., & Pöhlmann, S. (2026). Epidemiological and virological update on the emerging SARS-CoV-2 variant BA.3.2. The Lancet, Infectious Diseases, 26(1), e1–e2.

Zhang, Q. E., Lindenberger, J., Parsons, R. J., Thakur, B., Parks, R., Park, C. S., Huang, X., Sammour, S., Janowska, K., Spence, T. N., Edwards, R. J., Martin, M., Williams, W. B., Gobeil, S., Montefiori, D. C., Korber, B., Saunders, K. O., Haynes, B. F., Henderson, R., & Acharya, P. (2024). SARS-CoV-2 Omicron XBB lineage spike structures, conformations, antigenicity, and receptor recognition. Molecular Cell, 84(14), 2747–2764.e7.

Zhang, X., Jiang, L., Weng, G., Shen, C., Zhang, O., Liu, M., Zhang, C., Gu, S., Wang, J., Wang, X., Du, H., Zhang, H., Zhang, K., Wang, E., & Hou, T. (2025). HawkDock version 2: An updated web server to predict and analyze the structures of protein-protein complexes. Nucleic Acids Research, 53(W1), W306–W315.